*Desalination and Water Treatment*
www.deswater.com

doi: 10.5004/dwt.2019.23943

152 (2019) 26–32
June

# Investigation of natural Jordanian zeolite tuff (JZT) as adsorbent for TOC removal from industrial wastewater in a continuous fixed bed column: study of the influence of particle size

Waid Omar[a,*], Reyad Al Dwairi[b], Ziad S. Abu-Hamatteh[c], Nader Jabarin[b]

[a]*Department of Chemical Engineering, Faculty of Engineering Technology, Al-Balqa Applied University, P.O. Box 15008, Amman (11134), Jordan, Tel. +962792818634; email: waid.omar@bau.edu.jo*
[b]*Department of Natural Resources and Chemical Engineering, Tafila Technical University, P.O. Box 179, Tafila (6611), Jordan, emails: reyadn@hotmail.com (R.A. Dwairi), aljabarin@yahoo.com (N. Jabarin)*
[c]*Department of Civil Engineering, Faculty of Engineering Technology, Al-Balqa Applied University, P.O. Box 15008, Amman (11134), Jordan, email: hamatteh@bau.edu.jo*

Received 12 November 2018; Accepted 7 February 2019

**ABSTRACT**

Fixed bed column breakthrough curves are measured to evaluate the adsorption behavior of total organic carbon (TOC) from industrial wastewater onto natural Jordanian zeolite tuff (JZT). Two sizes fractions are studied, that is, 0.30–0.70 mm for JZT2 adsorbent and 0.70–1.0 mm for JZT1 adsorbent. Batch equilibrium experiments are conducted to determine the optimum pH for adsorption. The batch isotherms indicated that both JZT1 and JZT2 have higher adsorption capacity in the acidic environment at pH = 4. The measured breakthrough curves showed that the smaller size particle adsorbent exhibits enhanced column performance. The measured breakthrough curves are analyzed by Bohart–Adams, Thomas, Yoon–Nelson and Wolborska mathematical models. All the studied mathematical models fit the experimental breakthrough curves with $R^2 > 0.9$. The calculated adsorption capacity values using from Bohart–Adams are 25,956.28 and 22,472.39 mg/L for JZT2 and JZT1, respectively. Thomas rate constant values are 0.00042 L/min.mg for JZT2 and 0.00054 L/min.mg for JZT1. The estimated values from Yoon–Nelson model of the time needed to reach 50% of the breakthrough are 156.36 and 135.37 min for JZT2 and JZT1, respectively. The estimated kinetic coefficient values of the external mass transfer using Wolborska model are 7.22 $min^{-1}$ for JZT2 and 6.26 $min^{-1}$ for JZT1 adsorbent.

*Keywords:* TOC; Zeolite; Adsorption; Breakthrough curves; pH; Adsorption capacity; Particle size

## 1. Introduction

One of the current prime environmental concerns is the increase of the industrial activities that discharge wastewater effluents with dissolved organic pollutants, such as petroleum and petrochemical plants, coal liquefaction processes, pharmaceutical manufacturing, polymer industries and textile production [1–4]. Removal of such organic pollutants from wastewater before releasing it into the environment is a crucial issue [5–7]. The wastewater if not treated properly, the site or plant would not be able to discharge the water in compliance with environmental regulations [5–7].

Dissolved organic matter in wastewater is usually quantified using a measurable parameter called total organic carbon (TOC) which is well-known for describing the quality of municipal and industrial wastewaters in terms of organic pollutants. It is correlated to biological oxygen demand and chemical oxygen demand. Concentrations of organic matter in the effluent of wastewater treatment plants must be about 6–10 mg/L represented by its TOC [8].

Adsorption process was implemented as attractive, efficient and low-cost alternative for the separation of organic

* Corresponding author.

pollutants from industrial wastewater streams. Özdemir and Kılıç [9] investigated the potential use of agricultural waste for the removal of the organic pollutant methylene blue from wastewater. The results suggested that the agricultural waste has a high potential to be used as an effective adsorbent for MB adsorption. Activated carbon is a well-known adsorbent used in treating wastewater with organic pollutants, yet there were certain restrictions and limitations. Özdemir and Önal [10] prepared activated carbon using chemically activating polymer waste and evaluated the ability of the activated carbon in removing organic matter such as naproxen sodium, tannic acid and caffeine from aqueous solutions through a process of adsorption. Due to the fact that organic macromolecules are large in size, activated carbon exhibits slow mass transfer rates and therefore low efficiency [6,7]. Moreover, regeneration of activated carbon is an expensive process with limited usage in various industrial applicability [8]. Stoquart et al. [11] applied carbonized cedar wood chips (charcoal) as adsorbent to reduce TOC in wastewater. A good adsorption capacity of TOC onto charcoal was reported. Several research investigations on the use of clay materials as media of separating organic pollutants from waste streams have been reported with significant results as clay minerals are efficient and recyclable adsorbent [12–18].

Natural zeolites are plentiful and available at low-cost levels. Its structure is crystalline and porous containing numerous alumina-silicates hydrates. They exhibit a high cation exchange capacity and high capability to act as a molecular sieve. Natural zeolites have been extensively used as adsorbents in water purification processes [19–22]. It has been used in the adsorption of small organic pollutants from aqueous streams [23]. Zeolites (phillipsite and chabazite) exhibit a marked ability to absorb organic compounds such as humic acids from water [24]. In this work, natural Jordanian zeolite tuff (JZT) was investigated as a low-cost adsorbent for TOC removal from industrial wastewater in a continuous fixed bed column.

## 2. Materials and methods

### 2.1. Materials

The characterization of the adsorbent was discussed in detail by Özdemir and Önal [25]. They highlighted the most useful characteristics such as the pore properties including the Brunauer–Emmett–Teller surface area, the volume of the pore, its size distribution and average diameter. The impregnation ratio was determined as an important surface area property of the adsorbent along with Boehm titration, X-ray diffraction (XRD), fourier transform infrared, differential thermal analysis and thermal gravimetric analysis as important characterization methods [25].

The used adsorbent is a JZT collected from Mukawir volcano, Central Jordan. SEM analysis presented in Fig. 1 shows that the dominating zeolites in JZT are chabazite as major and phillipsite as minor minerals [26]. The JZT samples were analyzed for mineral composition using X-ray analysis (Fig. 2). Clearly, the X-ray analysis supports that chabazite as the major mineral in the JZT adsorbent.

JZT samples were subjected to crushing and sieving only, without any chemical modification. The samples were sieved into the size fraction (1.0–0.3 mm) which contains highest zeolite grade [26,27]. JZT samples were then sieved into two sizes: the size cuts (0.30–0.70 mm) for JZT2 adsorbent and (0.70–1.0 mm) for JZT1 adsorbent.

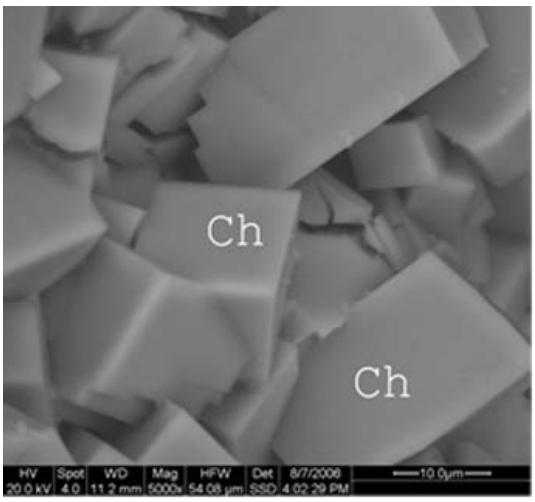


Fig. 1. SEM image of the natural Jordanian zeolitic tuff (JZT) adsorbent [26].

The wastewater stock was obtained from local industrial petrochemical industry. The wastewater stock was filtered using a filter paper of porosity 4 from the company Whatman, Fisher Scientific UK Ltd. (particle retention 12–25 mm) in order to remove all the suspended and undissolved matter. The sample was then analyzed for TOC three times to take an average value. The stock wastewater feed used in all experiments was from the same origin, which was stored in a closed opaque plastic vessel to prevent the exposure to the light. The TOC concentration of the wastewater stock used in all experiments was 83 mg/L.

### 2.2. Batch experiments

To determine the optimum pH that gives the optimum percentage removal (PR) of TOC for the two types of JZT adsorbents, different wastewater samples were prepared at different initial pH values by the addition of concentrated $HNO_3$ and NaOH solution. The range of pH investigated was from 3 (acidic medium) to 10 (basic medium). There was no precipitation or colloid formation observed at all the pH values. In each batch experiment, the initial pH value was adjusted at the desired value and measured at the start of the experiment. A 100 mL of the wastewater sample was mixed with 0.2 g of the JZT1 or JZT2 adsorbents in a tightly closed conical flask. The flask was covered by aluminum foil to ensure no light interactions and placed in a shaker for 6 h to reach equilibrium. The experiments were repeated three times in order to obtain accurate average values for both JZT1 and JZT2 at each pH of the solution. The percentage removal of TOC was then evaluated by measuring the final concentration of TOC. The percentage removal was calculated from the following equation:

$$\mathrm{PR} = \frac{C_i - C_f}{C_0} \times 100\% \quad (1)$$

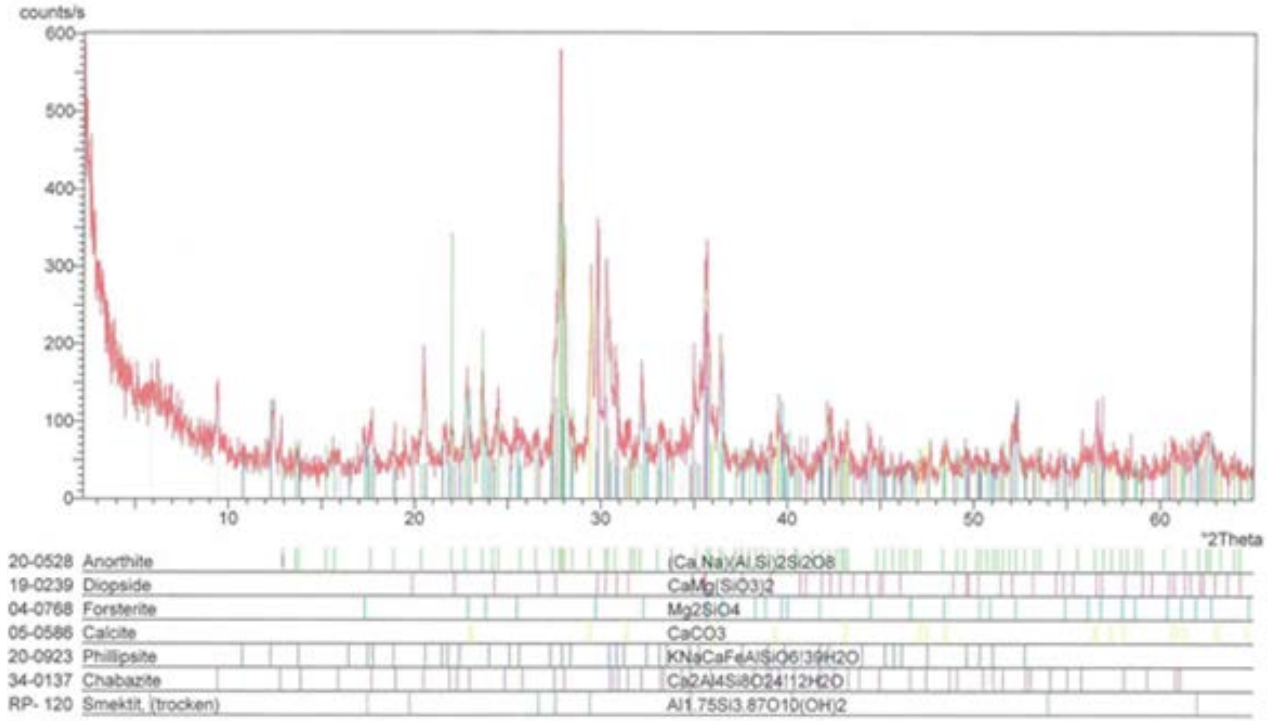


Fig. 2. XRD analysis for the natural Jordanian zeolitic tuff (JZT) adsorbent [26].

where $C_i$ is the concentration in the stock wastewater (83 mg/L), $C_f$ is the final equilibrium concentration.

### 2.3. Fixed bed adsorption experiments

The experimental setup used to measure the breakthrough curves for the continuous adsorption of TOC on the JZT absorbent is shown in Fig. 3. The influent was stored in a well closed 20 L feed tank. The glass column (50 cm length) is a cylindrical tube with a diameter of 1.13 cm equivalent to cross sectional area of 1 $cm^2$. The adsorbent was packed inside the column until the desired bed height is obtained. Fiber glass wool layers were fixed at the top and bottom of the backing to support the bed and protect it from being lost with the flowing solution. This support was observed and checked during the whole run. A peristaltic pump (Heidolph, Germany) was installed to force the liquid to flow downward through the column. The flow rate was kept constant at 50 mL/min for all experiments with a superficial velocity of 50 cm/min. The effluent from the column was collected and samples were taken at regular intervals to be analyzed for concentration measurements. The predetermined optimum pH value (acidic pH = 4) from equilibrium batch runs was selected for the fixed bed continuous runs.

### 2.4. TOC analysis

The TOC concentration of the filtered stock effluent was measured by indirect methods. The difference between the total carbon and the inorganic carbon was determined. TOC-VCPN instrument (Shimadzu, Japan) was used for the analysis. The system included an auto sampler ASI-V and an NDIR detector.

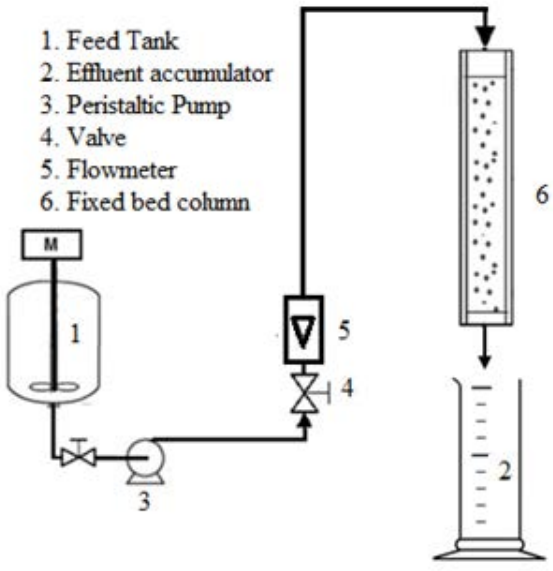


Fig. 3. Experimental setup used in the measurement of breakthrough curves.

## 3. Results and discussion

### 3.1. Influence of pH

The influence of pH value of the wastewater on the adsorption of TOC was investigated by using batch equilibrium experiments. Fig. 4 shows the PR of TOC for both JZT1 and JZT2 adsorbents over the pH range from 3 to 10. The pH

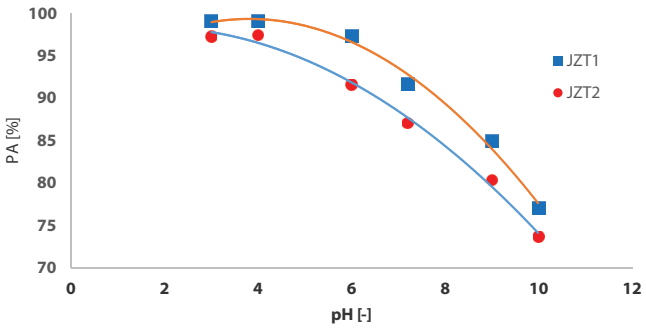


Fig. 4. Measured percentage adsorption of TOC on JZT1 and JZT2 adsorbents at different initial pH values using batch equilibrium experiments ($C_0$ = 83 mg/L, 0.2 g adsorbent/100 mL wastewater).

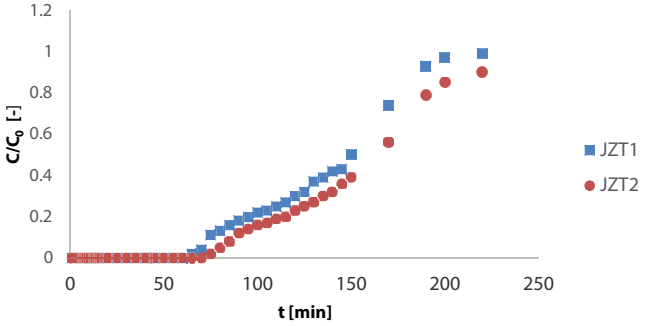


Fig. 5. Experimental breakthrough curves for TOC adsorption onto JZT1 and JZT2 adsorbents (bed height = 25 cm; flow rate = 50 mL/min; initial pH = 4; TOC concentration = 83 mg/L).

of the wastewater stock solution without any addition is 7.2. The results shown in Fig. 4 indicate that pH has a great impact on the adsorption of the TOC pollutants onto JZT. Higher removal percentage was measured in the acidic medium (pH = 4). The pH value plays an important role in changing the surface charge of zeolite [28–33]. The higher adsorption capacity in the acidic medium can be attributed to the effect of $H^+$ on decreasing the negative charge density in the pores, thus making the negative charge sites far apart with lower density. This will facilitate the diffusion of the organic macromolecules that are large in size (with more negative sites) into the pores and making a complexation with the hydrophilic sites of zeolite (metal ions). The measured higher adsorption capacity for the JZT in the strong acidic medium indicated that the protons adsorbed to the surface and improve the adsorption of TOC onto zeolite.

### 3.2. Fixed bed adsorption column

The performance of a fixed bed adsorption column is usually characterized by measuring breakthrough curve. The shape of the curve as well as the time to reach the breakthrough is very important features used in the design and operation of the adsorption column.

Continuous fixed bed column experiments were performed to determine the operating parameters for the adsorption process of TOC onto the JZT1 and JZT2 adsorbents. The two adsorbents JZT1 and JZT2 have the same origin and composition. However, they vary simply in their particle size with JZT1 is larger in particle size (0.70–1.0 mm) than JZT2 (0.30–0.70 mm). The experiments were conducted in a way that breakthrough curves can be obtained under controlled experimental conditions. All the parameters were kept constant (bed height = 25 cm; flow rate = 50 mL/min, initial pH = 4, TOC concentration = 83 mg/L) for both JZT1 and JZT2 adsorbents. The experimentally measured breakthrough curves are illustrated in Fig. 5.

The measured breakthrough curves show typical S shaped form (Fig. 5). This is a clear evidence that resistance to bulk diffusion mass transfer and the bonding of molecules into the pores surface play an important role during the adsorption process of TOC onto zeolite adsorbent. The measurements presented indicate a better column performance for TOC adsorption onto the smaller size adsorbent (JZT2) than the larger size adsorbent (JZT1). Thus, the time needed to reach the breakthrough time increases for smaller size particles (Fig. 5). It is well recognized that larger size adsorbent particles exhibits longer diffusion paths and therefore the molecules will be subjected to more resistance to be adsorbed to the active sites of the pores. Additionally, the available surface area for liquid–solid interface is greater in the case of smaller size particles, which plays an important role in the improvement of adsorption process.

### 3.3. Modeling of fixed bed breakthrough curves

For adsorption column design, the kinetic parameters need to be determined. In this study, four kinetic models, Adams–Bohart, Thomas, Yoon–Nelson and Wolborska, were applied to the measured experimental data to predict the breakthrough curves. These models were applied by Özdemir [34] for the removal of methylene blue by activated carbon in a fixed bed column.

#### 3.3.1. Bohart–Adams model

Bohart–Adams model is a commonly used mathematical model for the design of fixed bed adsorption columns [35,36]. It assumes that the adsorption process follows a rectangular isotherm and the rate of adsorption is proportional to the capacity of the adsorbent and the adsorbate concentration. A simple known linear form of Bohart–Adams model is given by the following relation [37]:

$$\ln\left(\frac{C_0}{C}-1\right)=\frac{K_{AB}N_0H}{V_0}-K_{AB}C_0t \quad (2)$$

where $C_0$ is the inlet concentration (mg/L), $C$ is the effluent concentration (mg/L), $K_{AB}$ is the Bohart–Adams kinetic constant (L/mg min), $V_0$ is the linear velocity (flow rate/column section area, cm/min), $H$ is the bed height (cm) and $N_0$ is the adsorption capacity of the adsorbent per volume of the bed (mg/L).

The linear fit of the experimental breakthrough curves according to Bohart–Adams model can be used to estimate the Bohart–Adams model parameters $K_{AB}$ and $N_0$. The calculated Bohart–Adams model parameters are given in Table 1. The change of the values of the parameters in Table 1 is resulted

Table 1
Parameters of Bohart–Adams, Thomas, Yoon–Nelson and Wolborska models using linear regression analysis of the experimental breakthrough curves

| Kinetic model parameters | Adsorbent | |
|---|---|---|
| | JZT2 | JZT1 |
| *Bohart–Adams* | | |
| $K_{AB}$ (L/mg min) | 0.000539 | 0.000431 |
| $N_0$ (mg/L) | 25,956.28 | 22,472.39 |
| $R^2$ | 0.9460 | 0.9376 |
| *Thomas* | | |
| $K_T$ (L/mg min) | 0.000421687 | 0.000542169 |
| $q$ (mg/g) | 26.54956571 | 21.18418222 |
| $R^2$ | 0.9186 | 0.9237 |
| *Yoon–Nelson* | | |
| $K_{YN}$ (1/min) | 0.0358 | 0.0447 |
| τ (min) | 156.36 | 135.37 |
| $R^2$ | 0.9301 | 0.9136 |
| *Wolborska* | | |
| $\beta_a$ (1/min) | 7.2262 | 6.2652 |
| $N_0$ (mg/L) | 34,669.05 | 33,121.75 |
| $R^2$ | 0.9448 | 0.9631 |

solely from the change of particle size of the adsorbent as all the operating parameters (flow rate, sorbate concentration, bed height and pH) were kept constant.

From the results of Table 1, the values of $N_0$ which represents the bed capacity per unit volume is higher for the smaller particle size adsorbent (JZT2). The values of $K_{AB}$ also increased with decreasing the particle size. The value of $K_{AB}$ usually increases with increasing process parameters that augment the external mass transfer rate [38] such as initial adsorbate concentration and the volumetric flow rate, which was fixed for both JZT1 and JZT2. This indicated that smaller size particles have a dominant role in enhancing the external mass transfer rate.

The linear regression $R^2 > 0.93$ show an overall good fit of the measured breakthrough curves to Bohart–Adams model. The calculated breakthrough curves from Bohart–Adams model compared with the experimentally measured data are depicted in Fig. 6. As shown in Fig. 6, the Bohart–Adams model smooths the experimental breakthrough curve at the initial part of the curve more accurately than the later part which is well known in the literature. This points out that the fixed bed adsorption process of TOC on the zeolite tuff used in this study can be limited by the external mass transfer and the design of the column can be performed based on the using Bohart–Adams model with excessive confidence.

### 3.3.2. Thomas model

Thomas model is of mostly used to model the breakthrough curves and to describe the performance of the fixed bed adsorption column. In addition, it estimates the adsorption capacity per one gram of the adsorbent, which is very important in the design of a continuous fixed bed adsorption column. Thomas model assumes adsorption with Langmuir isotherm with no axial dispersion. The model was derived on the basis that the rate driving force follows second order reaction kinetics [38–41]. Theoretically, it is suitable to estimate the adsorption process where the external and internal resistances to diffusion are very small [38]. The linearized form of Thomas model can be described by the following equation:

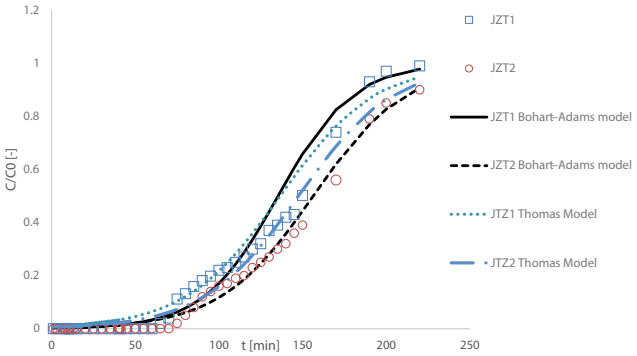


Fig. 6. Calculated breakthrough curves by Bohart–Adams and Thomas models compared with the measured experimental data.

$$\ln\left(\frac{C_0}{C}-1\right)=-\frac{C_0K_T}{F}\times V+\frac{M\times q\times K_T}{F} \tag{3}$$

where $F$ is the volumetric feed flow rate (mL/min), $K_T$ is Thomas rate constant (L/min.mg), $V$ is the volume of effluent wastewater (mL), $q$ maximum adsorption capacity (mg/g), $M$ is the adsorbent mass in the column (g).

The Thomas model parameters ($K_T$ and $q$) were determined by the linear fitting of the experimental data according to Eq. (3). The Thomas model parameters were calculated from the slopes and intercepts of linear plot of $\ln\left(\frac{C_0}{C}-1\right)$ against $t$. The Thomas model parameters are listed in Table 1.

The results presented in Table 1 indicate higher adsorbent capacity for smaller size adsorbent (JZT2) while the value of Thomas constant decreases. This is resulted from the higher driving force due to the smaller adsorbent size, which resulted in better column performance. The predicted breakthrough curves for both adsorbent sizes according to the Thomas model are displayed in Fig. 6. It is clear from Fig. 6 that Thomas model fits the experimental data very well only in the earlier part up to $C/C_0$ value of 0.3 of the breakthrough curve, while in the later part there were discrepancies from the experimental data.

### 3.3.3. Yoon–Nelson model

The Yoon–Nelson model assumes that the decreasing in the rate of adsorption probability is directly proportional to the probability of molecule adsorption and probability of molecule breakthrough. The Yoon–Nelson expression in its linear form is as follows [42]:

$$\ln\left(\frac{C}{C_0 - C}\right) = K_{YN}t - \tau K_{YN} \quad (4)$$

where $K_{YN}$ is the Yoon–Nelson rate constant (1/min) and τ is the time needed to reach 50% of the breakthrough (min).

The value of $K_{YN}$ depends on the column operating conditions such as initial adsorbate concentration, bed height and feed flow which were kept constant in this study and the experiments were conducted to understand the performance of the fixed bed column when loaded with small size and large size zeolite. The values of $K_{YN}$ and τ are estimated from the slopes and intercepts of the linear plot of $\ln\left(\frac{C}{C_0 - C}\right)$ against $t$ for the both adsorbents JZT1 and JZT2. The estimated Yoon–Nelson model parameters for both adsorbents are given in Table 1.

From the results listed in Table 1, it can be observed that the smaller size adsorbent (JZT2) exhibits better column performance. The increased value of $K_{YN}$ for the adsorbent of smaller size indicates increased driving force of mass transfer. In addition, the increase in τ with decreasing particle size points out that smaller size adsorbent reveals higher capacities. The estimated correlation coefficient $R^2$ values of 0.9136 and 0.9301 for JZT2 and JZT1 adsorbents, respectively, show a good fit of the experimental data to Yoon–Nelson model. The comparison of data from simulated Yoon–Nelson model breakthrough curves and the experimental data is illustrated in Fig. 7.

### 3.3.4. Wolborska model

The column performance can be well defined and understood in terms of mass transfer mechanism by applying Wolborska model [43]. The model is based on the general equation of mass transfer for the diffusion mechanism for low concentration ranges. The mass transfer in the fixed bed column can be described by the following linear equation:

$$\ln\left(\frac{C}{C_0}\right) = \frac{\beta_a C_0}{N_0} \times t - \frac{\beta_a H}{V_0} \quad (5)$$

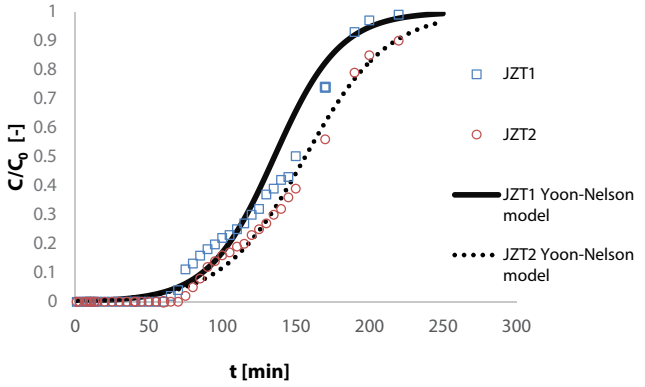


Fig. 7. Comparison of breakthrough curves calculated according to Yoon–Nelson model and the experimental values for the adsorption of TOC onto JZT1 and JZT2 adsorbents.

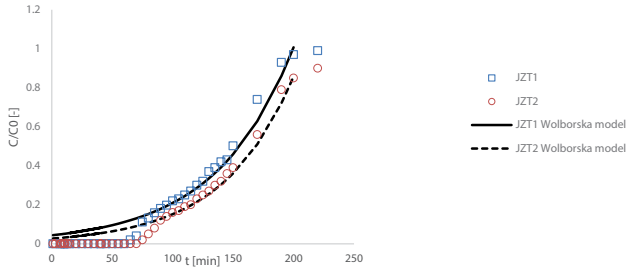


Fig. 8. Simulated breakthrough curves according to Wolborska model for the adsorption TOC onto JZT1 and JZT2 adsorbents compared with the measured breakthrough curves.

where $\beta_a$ is the kinetic coefficient of the external mass transfer (1/min). $N_0$ is the bed capacity per unit volume of the bed (mg/L). A linear plot of the experimental breakthrough measurements according to Eq. (5) is applied to extract the kinetic parameters. The calculated parameters are given in Table 1. Fig. 8 exemplifies the degree of fitting of Wolborska model to the measured breakthrough curves. However, in the initial stages, there is a clear divergence from the experimental data. The estimated values of the kinetic external mass transfer coefficient ($\beta_a$) is 7.22 and 6.26 $min^{-1}$ for JZT2 and JZT1 adsorbents, respectively. It is clear that smaller size adsorbent has higher diffusion mass transfer driving force. This also can be obviously concluded from the higher $N_0$ value for JZT2 given in Table 1 indicating increased adsorption capacity for smaller size adsorbent.

## 4. Conclusions

Jordanian natural zeolite tuff is investigated as a low-cost adsorbent to treat industrial wastewater with dissolved organic matter. The advantage of this adsorbent is its availability in large amounts and it could be implemented directly after crushing and sieving without any additional cost. The column performance results indicated that the natural zeolite could be suitable for industrial applications in wastewater treatment of effluents with organic pollutants. The particle size is found to be an influential parameter. However, it is recommended to conduct further research to modify the microstructure of the zeolite to modify the adsorption and thus the column performance.

## References

[1] D. Rajkuman, K. Planivelu, Electrochemical separation of cresols for wastewater treatment, Ind. Eng. Chem. Res., 42 (2003) 1833–1839.
[2] J. Blanco, F. Torrades, M. De la Varga, J. García-Montaño, Fenton and biological-Fenton coupled processes for textile wastewater treatment and reuse, Desalination, 286 (2012) 394–399.
[3] A. Asghar, A. Aziz, A. Raman, W. Mohd, A. Wan, Advanced oxidation processes for in-situ production of hydrogen peroxide/hydroxyl radical for textile wastewater treatment: a review, J. Clean. Prod., 87 (2015) 826–838.
[4] J. Lin, C.Y. Tang, W. Ye, S.P. Sun, S.H. Hamdan, A. Volodin, C. Van Haesendonck, A. Sotto, P. Luis, B. Van der Bruggen, Unraveling flux behavior of superhydrophilic loose nanofiltration membranes during textile wastewater treatment, J. Membr. Sci., 493 (2015) 690–702.

[5] M. Said, H. Abu Hasan, M. Tusirin, M. Nor, A. Mohammad, Removal of COD, TSS and colour from palm oil mill effluent (POME) using montmorillonite, Desal. Wat. Treat., 57 (2016) 10730–10744.
[6] C. Feng, J. Jin, L. Sun, Y. Zhang, X. Chen, X. Zhang, Study on the organics adsorption capacities of powdered activated carbon and activated coke in reclaimed water, Desal. Wat. Treat., 62 (2017) 200–207.
[7] S. Bekkouche, M. Bouhelassa, A. Ben Aissa, S. Baup, N. Gondrexon, C. Pétrier, S. Merouani, O. Hamdaoui, Synergy between solar photocatalysis and high frequency sonolysis toward the degradation of organic pollutants in aqueous phase - case of phenol, Desal. Wat. Treat., 62 (2017) 457–464.
[8] J. Hatt, E. Germain, S. Judd, Granular activated carbon for removal of organic matter and turbidity from secondary wastewater, Water Sci. Technol., 67 (2013) 846–53.
[9] Ç. Özdemir, F. Kılıç, Kinetics behavior of methylene blue onto agricultural waste, Part. Sci. Technol., 36 (2018) 194–201.
[10] Ç. Özdemir, Y. Önal, Study to observe the applicability of the adsorption isotherms used for the adsorption of medicine organics onto activated carbon, Part. Sci. Technol., 36 (2018) 254–261.
[11] C. Stoquart, P. Servais, P.R. Bérubé, B. Barbeau, Hybrid membrane processes using activated carbon treatment for drinking water: a review, J. Membr. Sci., 411 (2012) 1–12.
[12] J. Altmann, D. Rehfeld, K. Träder, A. Sperlich, M. Jekel, Combination of granular activated carbon adsorption and deep-bed filtration as a single advanced wastewater treatment step for organic micropollutant and phosphorus removal, Water Res., 92 (2016) 131–139.
[13] R. Toor, M. Mohseni, UV-$H_2O_2$ based AOP and its integration with biological activated carbon treatment for DBP reduction in drinking water, Chemosphere, 66 (2007) 2087–2095.
[14] A. Miura, E. Shiratani, I. Yoshinaga, T. Hitomi, K. Hamada, K. Takaki, Characteristics of the adsorption of dissolved organic matter by charcoals carbonized at different temperatures, Jpn. Agric. Res. Q.: JARQ, 41 (2007) 211–217.
[15] G.A. Garwood, M.M. Mortland, T.J. Pinnavaia, Immobilization of glucose oxidase on montmorillonite clay: hydrophobic and ionic modes of binding, J. Mol. Catal., 22 (1983) 153–163.
[16] T.A. Wolf, T. Demirel, R.E. Baumann, Adsorption of organic pollutants on montmorillonite treated with amines, J. Water Pollut. Control Fed., 58 (1986) 68–76.
[17] S.A. Boyd, M.M. Mortland, Selective effects of smectite-organic complexes on the activities of immobilized enzymes, J. Mol. Catal., 34 (1986) 1–8.
[18] K.R. Srinivasan, S.H. Fogler, Use of inorgano-organo-clay in the removal of priority pollutants from industrial wastewaters: adsorption of benzopyrene and chlorophenols from aqueous solutions, Clays Clay Miner., 38 (1990) 287–293.
[19] S. Kesraouiouki, C.R. Cheeseman, R. Perry, Natural zeolite utilization in Pollution control a review of applications to metals effluents, J. Chem. Technol. Biotechnol., 59 (1994) 121–126.
[20] A. Hedstrom, Ion exchange of ammonium in zeolites: a literature review, J. Environ. Eng.: ASCE, 127 (2001) 673–681.
[21] S. Babel, T.A. Kurniawan, Low-cost adsorbents for heavy metals uptake from contaminated water: a review, J. Hazard. Mater., 97 (2003) 219–243.
[22] D. Caputo, F. Pepe, Experiments and data processing of ion exchange equilibria involving Italian natural zeolites: a review, Microporous Mesoporous Mater., 105 (2007) 222–231.
[23] H.T. Shu, D. Li, A.A. Scala, Y.H. Ma, Adsorption of small organic pollutants from aqueous streams by aluminosilicate-based microporous materials, Sep. Purif. Technol., 11 (1997) 27–36.
[24] L. Ambrosone, S. Canzano, P. Iovino, S. Salvestrini, S. Capasso, C. Colella, A phenomenological interpretation of twostep adsorption kinetics of humic acids on zeolitic tuff, Adsorpt. Sci. Technol., 31 (2013) 373–384.
[25] Ç. Özdemir, Y. Önal, Synthesis of new activated carbons produced from polymer waste, Fullerenes Nanotubes Carbon Nanostruct., 26 (2018) 451–457.
[26] R.A. Al Dwairi, Characterization of the Jordanian Zeolitic Tuff and Its Potential Use in Khirbet es Samra Wastewater Treatment Plant. PhD Thesis, The University of Jordan, Amman, Jordan, 2007.
[27] R.A. Al Dwairi, K.M. Ibrahim, H.N. Khoury, Potential use of faujasite–phillipsite and phillipsite–chabazite tuff in purification of treated effluent from domestic wastewater treatment plants, Environ. Earth Sci., 71 (2014) 5071–5078.
[28] M. Kithome, J.W. Paul, L.M. Lavkulich, A.A. Bomke, Effect of pH on ammonium adsorption by natural zeolite clinoptilolite, Commun. Soil Sci. Plant Anal., 30 (1999) 1417–1430.
[29] J. Lemić, S. Milošević, M. Vukašinović, A. Radosavljević–Mihajlović, D. Kovaćević, Surface modification of a zeolite and the influence of pH and ionic strength on the desorption of an amine, J. Serb. Chem. Soc., 71 (2006) 1161–1172.
[30] A. Heidari, H. Younesi, Z. Mehrabanb, H. Heikkinen, Selective adsorption of Pb (II), Cd(II), and Ni(II) ions from aqueous solution using chitosan-MAA nanoparticles, Int. J. Biol. Macromol., 61 (2013) 251–263.
[31] M.W. Munthali, P. Kabwadza-Corner, E. Johan, N. Matsue, Decrease in cation exchange capacity of zeolites at neutral pH: examples and proposals of a determination method, J. Mater. Sci. Chem. Eng., 2 (2014) 1–5.
[32] P. Kabwadza-Corner, E. Johan, N. Matsue, pH dependence of lead adsorption on zeolites, J. Environ. Prot., 6 (2015) 45–53.
[33] R. Ghemit, M. Boutahala, A. Kahoul, Removal of diclofenac from water with calcined ZnAlFe-$CO_3$ layered double hydroxides: effect of contact time, concentration, pH and temperature, Desal. Wat. Treat., 83 (2017) 75–85.
[34] Ç. Özdemir, Removal of methylene blue by activated carbon prepared from waste in a fixed-bed column, Part. Sci. Technol., 32 (2014) 311–318.
[35] K.H. Chu, Fixed bed sorption: Setting the record straight on the Bohart–Adams and Thomas models, J. Hazard. Mater., 177 (2010) 1006–1012.
[36] D.O. Cooney, Adsorption Design for Wastewater Treatment, Lewis Publishers, Boca Raton, 1999.
[37] G.S. Bohart, E.Q. Adams, Some aspects of the behavior of charcoal with respect to chlorine, J. Am. Chem. Soc., 42 (1920) 523–529.
[38] Z. Aksu, F. Gonen, Biosorption of phenol by immobilized activated sludge in a continuous packed bed: prediction of breakthrough curves, Process Biochem., 39 (2004) 599–613.
[39] H.C. Thomas, Heterogeneous ion exchange in a flowing system, J. Am. Chem. Soc., 66 (1944) 1664–1666.
[40] J. Wu, H.Q. Yu, Biosorption of 2,4-dichlorophenol from aqueous solutions by immobilized *Phanerochaete chrysosporium* biomass in a fixed bed column, Chem. Eng. J., 138 (2008) 128–135.
[41] S. Ayoob, A.K. Gubta, P.B. Bhakat, Analysis of breakthrough developments and modeling of fixed bed adsorption system for As (V) removal from water by Modified Calcined Bauxite (MCB), Sep. Purif. Technol., 52 (2007) 430–438.
[42] Y.H. Yoon, J.H. Nelson, Application of gas adsorption kinetics. I. A theoretical model for respirator cartridge surface time, Am. Ind. Hyg. Assoc. J., 45 (1984) 509–516.
[43] A. Wolborska, Adsorption on activated carbon of p-nitrophenol from aqueous solution, Water Res., 23 (1989) 85–91.